

Feedback Induced Instability and Chaos in Semiconductor Lasers and Their Applications

Junji OHTSUBO

Faculty of Engineering, Shizuoka University, 3-5-1, Johoku, Hamamatsu, 432-8561 Japan

(Received November 4, 1998; Accepted November 13, 1998)

Semiconductor laser with feedback is an excellent model for nonlinear optical system which shows chaotic dynamics. It is interesting not only from the fundamental physical study but also application standpoints of view. The dynamics of feedback induced instability and chaos, especially for optical feedback, and their applications are reviewed in this paper. The model of such a system is described by the laser rate equations. At first the dynamic behaviors of feedback induced instability and chaos in semiconductor lasers are discussed on the basis of the theory and experiments. Instability and chaos may be stabilized by the method of chaos control. Then we apply the method to suppress the noise induced by the feedback in a semiconductor laser. The synchronization of chaos between two similar systems is also an important issue in chaos applications and we discuss secure communications based on chaos synchronization. Some other examples of applications of feedback induced chaos are also described.

Key words: semiconductor laser, optical feedback, instability and chaos, chaos control, chaos synchronization, application of chaos

1. Introduction

The study of instability and chaos in optics goes back to the middle of '70s when it was proved that the laser rate equations can be described by the similar differential equations to the chaos model developed by Lorenz.¹⁾ In the mean time, chaotic behaviors were demonstrated in a ring laser system.²⁾ Since early '80s, feedback induced instability and chaos in semiconductor lasers have also been paid much attention as one of the most interesting nonlinear phenomena in optics.³⁾ Here "feedback" means not only optical one from an external reflector outside the laser cavity, but also an opto-electronic one through a photodetector to the injection current. In this review, we are mainly concerned with optical feedback effects in semiconductor lasers.

When the light reflected from an external reflector couples with the original field in the laser cavity, the laser oscillation is affected considerably. A variety of dynamical behaviors can be observed in semiconductor lasers with optical feedback and they have been investigated by many researchers for those two decades. One of the main differences between semiconductor lasers and other lasers is low reflectivities of the internal mirrors in the laser cavity. It ranges typically only from 10 to 30% of the intensity in Fabry-Perot semiconductor lasers. This makes the feedback effects significant in semiconductor lasers. Other difference is a large absolute value of the linewidth enhancement factor α . The value of $\alpha = -2$ to -6 was reported in semiconductor lasers, while this value is almost zero in other lasers. These facts lead to interesting and a variety of dynamics different from other lasers. At weak to moderate optical feedback reflectivity, the output power of the laser shows interesting dynamical

behaviors such as stable state, periodic and quasi-periodic oscillations, and chaos with the change of the system parameters. These ranges of the external reflectivity are not only interesting but also very important in actual applications of semiconductor lasers such as in optical data storage systems. The dynamical behaviors of a semiconductor laser with optical feedback are mainly influenced by three parameters in the system, which include the reflectivity and length of the external mirror and the bias injection current. Extensive lists of the literature for the dynamic characteristics in semiconductor lasers with optical feedback in early times can be found in Refs. 4) and 5).

The dynamic behaviors of a semiconductor laser with optical feedback are not simple and strongly dependent on the feedback reflectivity. According to the behaviors of the laser output, the dynamics of the output power can be characterized into five regimes (I-V) with increase of the feedback reflectivity.^{6,7)} For the very small feedback regime I, the laser linewidth is increased or decreased depending on the phase of the returned light into the laser cavity. With increase of the feedback level, the laser shows mode hopping among several external cavity modes (regime II). Chaos can be observed at moderate levels of the feedback amplitude reflectivity around 1% which corresponds to the regimes III and IV. With further increase of the feedback level, coherence collapse occurs in the laser output power, in which the linewidth is drastically broadened and the coherence length of the laser is much reduced. These regions are very important in actual optical data storage systems. A very high feedback level (regime V) corresponds to stable laser operation. We are much interested in the regimes III and IV which show chaotic dynamics and the detailed descriptions in these regimes are presented in the following.

Up to now, a lot of semiconductor laser devices with

E-mail: ohtsubo@eng.shizuoka.ac.jp

different structures have been proposed and fabricated. In spite of the differences of device structures, the dynamics of semiconductor lasers are the same as long as the laser rate equations are written by the same or similar forms. For those two decades, the dynamic behaviors of semiconductor lasers with optical feedback and their related topics have been investigated and a lot of fruitful results have been obtained. Yet, the phenomena contain much of fundamental physics and the study is still under way. Optical feedback effect is an old problem but it is still an important issue in semiconductor lasers. The fundamental study of chaotic dynamics was the main issue for the semiconductor lasers with optical feedback, but the situation has been changed in early '90s. The ideas of the control and synchronization of chaos have been proposed and developed for the decade. Namely, applications of chaos have been opened by these methods. Of course, many applications of chaos have been proposed and demonstrated in semiconductor lasers with optical feedback.

In this review, we start from the brief description of the general laser rate equations which reduce to the Lorenz equations and the classifications of lasers are given. A semiconductor laser is a class B laser and it does not show chaotic dynamics, but it is easily destabilized by external disturbances such as external feedback and, as a result, shows chaotic dynamics. The theoretical background of semiconductor lasers with optical feedback is described by the rate equations and the stability and instability are studied by the linear stability analysis for the equations. In this review, instability and chaos in that system are demonstrated by the numerical simulations based on the rate equations and the linear stability analysis, and some experimental results are presented. Routes to chaos in this system have been clarified at certain extents and we will discuss them in details. Phase conjugate optical feedback is also an interesting issue in semiconductor lasers since a semiconductor laser is recently used as a light source in phase conjugate optics. The different dynamics from those for conventional mirror feedback are expected in phase conjugate feedback and we will present some of the effects. As applications of chaos, the methods of the control of chaos and the chaos synchronization between two similar systems are introduced and some applications are demonstrated. Most of the descriptions in this reviews are concerned with those for Fabry-Perot single mode lasers. But, finally, the dynamics and applications for some of new types of semiconductor lasers such as VCSELs (vertical-cavity surface-emitting lasers) and high power semiconductor lasers are also briefly described.

2. Theory of Semiconductor Lasers with Optical Feedback

The theoretical approach for laser dynamics is based on the rate equations. Various laser models by using the rate equations have been proposed up to present. Here, as a starting point, we employ a Haken model which

describes a unidirectional ring laser.^{1,5)} The rate equations of this model proves to be reduced to the same differential equations as those of the well known Lorenz model in chaotic dynamics. Next, the rate equations of semiconductor lasers with optical feedback are introduced. The stability and instability of laser oscillation can be theoretically discussed by the linear stability analysis for the rate equations. We also treat this analysis.

2.1 Lorenz-Haken Model of Lasers

Starting from Maxwell's equation of the laser field in a unidirectional ring laser model with a two level system and using a slowly-varying-envelope approximation, after some calculations, the equations for the laser field A , the polarization B , and the power gain per unit length g are written by^{1,5)}

$$\frac{dA}{dt} = \frac{i}{2} v_0 B - \frac{1}{2\tau_p} A, \quad (1)$$

$$T_2 \frac{dB}{dt} = -(1 - i\delta)B - igA, \quad (2)$$

$$T_1 \frac{dg}{dt} = (g_0 - g) + \frac{\text{Im}[A^*B]}{I_{\text{sat}}}. \quad (3)$$

These equations are called the Haken equations and derived as a mean field limit. Here, v_0 is the speed of light in the medium, δ is the scaled atomic detuning, g_0 is the small signal gain, and I_{sat} is the intensity saturation. τ_p is the photon lifetime, T_1 is the population decay time, and T_2 is the dipole dephasing time. It is easily shown by appropriate scalings for the variables that the Haken equations reduce to the Lorenz equations which show chaotic dynamics. Therefore, Eqs. (1)–(3) are called the Lorenz-Haken equations.^{1,5)}

Since chaotic dynamics are expected to be occurred in the existence of three coupled, first-order, nonlinear differential equations, a laser described by Eqs. (1)–(3) can be a candidate which shows instability and chaos in its output. However, in actual, the polarization equation or the polarization and gain equations may be eliminated due to small scales of the lifetimes. Depending on such categories, lasers are classified into three types, namely, A, B, and C classes.⁵⁾ In class A lasers, for example, He-Ne laser and dye lasers, the lifetimes T_1 and T_2 are so small compared with the photon lifetime τ_p . Therefore, both the polarization and population inversion equations are adiabatically eliminated and only the field equation becomes the important term. As a result, chaotic dynamics cannot be observed in class A lasers. In class B lasers, for example, CO₂ laser and semiconductor laser, only the polarization equation can be adiabatically eliminated due to the small lifetime of T_2 . Therefore, class B lasers are also not candidates which show chaotic dynamics. The field equation contains amplitude and phase. At glance, class B lasers are described by three nonlinear differential equations (amplitude, phase, and gain) and they are supposed to show chaotic dynamics. But it is easily proved that the phase equation is decoupled from other two, so that class B lasers themselves cannot exhibit

chaos. But class B lasers easily exhibit instability and chaos when one more degree of freedom is introduced to them. A degree of freedom to be added may be an external injection or an optical feedback from an external reflector. This induces coupling between the phase and the amplitude and the system is capable of exhibiting chaotic dynamics. In class C lasers, for example, far-infrared NH_3 laser and Ar ion laser, all three equations in Eqs. (1)–(3) must be considered and such lasers show chaotic dynamics under appropriate conditions without any external disturbance or modulation.

2.2 Semiconductor Lasers with Optical Feedback

Semiconductor laser is not simply modeled by a two-level system as discussed in the previous section, but the approximations^{5,8)} lead to two differential equations with the complex field and the carrier density. In the presence of optical feedback, the feedback term is added to the field equation. Figure 1 shows a schematic of a semiconductor laser with optical feedback. We assume the same reflectivities for the rear and front facets of the laser, but a different case is a straightforward extension. As already stated, the field amplitude is coupled with the phase due to optical feedback, so that various dynamic behaviors related to instability and chaos are expected to the laser output power. The theoretical study for the dynamic characteristics of semiconductor lasers with optical feedback is performed based on these rate equations. Assuming that the laser oscillates in a single longitudinal mode with an angular frequency ω_0 , the complex electric field in the active region is written as $E(t) \exp[i(\omega_0 t + \phi(t))]$, where $\phi(t)$ is the phase change of the field. Then, the rate equations for the amplitude and phase of the complex electric field and the carrier density are given by^{3,9,10)}

$$\frac{dE(t)}{dt} = \frac{1}{2} \left\{ G(N(t) - N_0) - \frac{1}{\tau_p} \right\} E(t) + \frac{\kappa}{\tau_{in}} E(t - \tau) \cos \theta(t) + F_E(t), \quad (4)$$

$$\frac{d\phi(t)}{dt} = \frac{\alpha}{2} \left\{ G(N(t) - N_0) - \frac{1}{\tau_p} \right\} - \frac{\kappa}{\tau_{in}} \frac{E(t - \tau)}{E(t)} \sin \theta(t) + F_\phi(t), \quad (5)$$

$$\frac{dN(t)}{dt} = J - \frac{N(t)}{\tau_s} - G \{ N(t) - N_0 \} |E(t)|^2 + F_N(t), \quad (6)$$

where G is the linear gain coefficient, N_0 is the carrier density at transparency, α is the linewidth enhancement factor, and J is the injection current density. τ_p is the photon life time as already introduced, τ_s is the carrier life time, $\tau = 2L/c$ is the external cavity round-trip time where L is the distance from the laser facet to the external reflector and c is the light velocity in vacuum, and $\tau_{in} = 2\eta l/c$ is the round-trip time within the laser cavity where l is the internal cavity length and η is the refractive index of the laser cavity. The Langevin noise terms F_E , F_ϕ , and F_N are included in the rate equations. $\theta(t)$

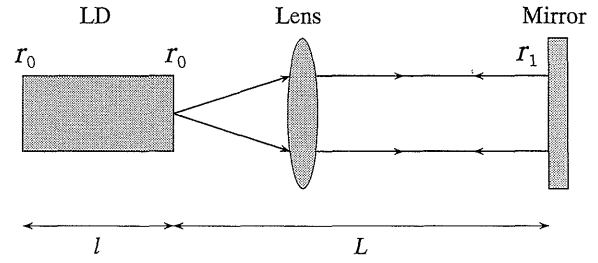


Fig. 1. Schematic diagram of semiconductor laser with optical feedback.

represents the phase coupling between the original light in the cavity and the delayed light from the external reflector, and is given by the following form

$$\theta(t) = \omega_0 \tau + \phi(t) - \phi(t - \tau). \quad (7)$$

The feedback parameter κ is written by $\kappa = (1 - r_0^2)r/r_0$, where r_0 and r are the amplitude reflectivities of the laser exit facet and the external reflector, respectively. Since multiple reflections between the laser facet and the external reflector are neglected, Eqs. (4)–(7) are valid for a weak to moderate feedback level. Choosing appropriate values of the system parameters such as the injection current J , the external reflectivity r , and the external cavity length L , Eqs. (4)–(7) are numerically solved. The fourth order Runge-Kutta algorithm is frequently used since the laser output power signal rapidly changes in time. In the following numerical simulations, we use the same parameter values listed in Table 1 in Ref. 11).

2.3 Linear Stability Analysis

Next, we briefly describe the linear stability analysis for Eqs. (4)–(7) for the study of stable oscillation conditions of the laser output power. The linear stability analysis has already been given in detail in the references.^{12,13)} For the calculation of linear stable modes, we at first derive the stationary solutions for the variables. We assume the solutions for the amplitude, the phase, and the carrier density as $E(t) = E_s$, $\phi(t) = (\omega_s - \omega_0)t$, and $N(t) = N_s$, respectively. Inserting these solutions into Eqs. (4)–(7), the stationary solutions for each variable can be obtained in the following forms.

$$G(N_s - N_0) - \frac{1}{\tau_p} = -2 \frac{\kappa}{\tau_{in}} \cos \omega_s \tau, \quad (8)$$

$$\omega_s - \omega_0 = -\frac{\kappa}{\tau_{in}} (\alpha \cos \omega_s \tau + \sin \omega_s \tau), \quad (9)$$

$$G(N_s - N_0) E_s^2 = J - \frac{N_s}{\tau_s}. \quad (10)$$

The laser oscillation angular frequency is proportional to the injection current and written by

$$\omega_0 = \omega_c - \frac{\partial \omega_0}{\partial J} J, \quad (11)$$

where ω_c is the constant angular frequency at a certain bias injection current and $\partial \omega_0 / \partial J$ is the angular fre-

quency conversion efficiency to the injection current. The relation between the solitary laser angular frequency ω_0 and the laser angular oscillation frequency ω_s for the steady state condition is given by^{3,13}

$$(\omega_0 - \omega_s)\tau = C \sin(\omega_s\tau + \arctan \alpha), \quad (12)$$

with

$$C = \frac{\kappa\tau}{\tau_{in}} \sqrt{1 + \alpha^2}. \quad (13)$$

In Eq. (12), the laser angular oscillation frequency ω_s generally has multiple solutions and the number of solutions depends on the parameter value C . The actual laser oscillation is determined both from the phase and gain conditions for the stable state. For a larger value of C , the laser becomes unstable and it sometimes hops around among possible oscillation frequencies. From Eqs. (8)–(10), the angular frequency shift $\Delta\omega_s = \omega_s - \omega_0$ and the carrier density N_s lie on an ellipse and stable and unstable natures of the laser oscillation, such as Hopf and saddle node bifurcations, can be discussed by the locations of the solutions.^{5,14} Among multiple solutions, we choose one that results in the maximum gain as a steady state solution for the angular frequency in the following numerical calculations, however, it is noted that it is not always true in actual situation of laser oscillation.

In order to analyze the stability of the laser output power for a small perturbation from the stationary state, we assume the form of the solutions in the rate equations as

$$x(t) = x_s + \delta x \exp(\gamma t) \quad (x = E, N, \phi), \quad (14)$$

where $\gamma (= \Gamma + i\Omega)$ is a complex number. The real and imaginary parts of γ represent the amplitude damping rate and the frequency of the small perturbation, respectively. Therefore, a solution diverges for the case of $\Gamma > 0$ with time evolution, while it converges for the case of $\Gamma < 0$. Substituting the stationary solutions with small perturbations into the rate equations, one obtains the following characteristic equation for γ ^{10,12,13}

$$\begin{aligned} D(\gamma) = & \gamma^3 + \gamma^2 \left[\frac{1}{\tau_R} + \frac{2\kappa A}{\tau_{in}} \cos(\omega_s\tau) \right] \\ & + \gamma \left[\omega_R^2 + \frac{2\kappa A}{\tau_R \tau_{in}} \cos(\omega_s\tau) + \left(\frac{\kappa A}{\tau_{in}} \right)^2 \right] \\ & + \left\{ \frac{1}{\tau_R} \left(\frac{\kappa A}{\tau_{in}} \right)^2 + \omega_R^2 \frac{\kappa A}{\tau_{in}} [\cos(\omega_s\tau) - \alpha \sin(\omega_s\tau)] \right\} \\ = & 0, \end{aligned} \quad (15)$$

with $A = 1 - \exp(\gamma\tau)$, $B = 1 + \exp(\gamma\tau)$, and $\tau_R^{-1} = \tau_s^{-1} + gE_s^2$, where $\omega_R = 2\pi f_R$ ($\omega_R^2 = gE_s^2/\tau_p$) is the relaxation oscillation angular frequency of the solitary laser. Stable oscillation conditions of the laser output are studied by stable linear modes corresponding to the solutions of the above equation. As discussed in later, the relaxation oscillation frequency plays an important role for the laser dynamics. The relaxation oscillation frequency for the solitary laser is calculated from the characteristic equation without optical feedback (by setting $\kappa = 0$). For no exter-

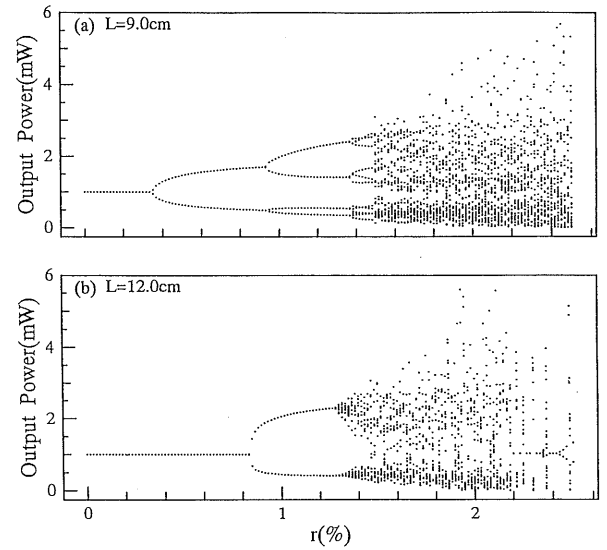


Fig. 2. Calculated bifurcations of the laser output power for variations of the external reflectivity at $J=1.3J_{th}$. The external cavity lengths are (a) $L=9.0$ and (b) 12.0 cm. (a) period doubling bifurcation and (b) quasi-periodic bifurcation.

nal feedback, the relaxation oscillation of the laser output power is originated from statistical Langevin noises involved in the rate equations in Eqs. (4)–(6). But it is much enhanced by the mixing of the original laser oscillation with an external feedback light.

3. Instability and Chaos

Many theoretical and experimental researches for instability and chaos in semiconductor lasers with optical feedback have been performed up to now.^{15–19} The theoretical study is based on the rate equations and the linear stability analysis as described in the previous section. Here, we demonstrate some of results from our studies.

3.1 Chaotic Bifurcations

It is a common practice to investigate bifurcation scenarios for a variable of interest in a chaotic system. The variable to be investigated is the laser output power and the system parameters to be varied are the reflectivity and length of the external mirror and the injection current in our case. There are three typical bifurcation scenarios in semiconductor lasers with optical feedback.^{5,20–23} The first is a route to chaos with period doubling bifurcation and the second is a quasi-periodic bifurcation route. The third one is an intermittent bifurcation which is much related to low frequency fluctuation discussed in later. Here, we discuss the first two types of chaos. Figure 2 shows examples of bifurcations of the laser output power for variation of the external reflectivity calculated from numerical simulations for the rate equations. The external cavity lengths are $L=9.0$ and 12.0 cm for Figs. 2(a) and (b), respectively. The injection current is fixed to be $J=1.3J_{th}$. Figure 2(a) corresponds to period doubling bifurcation as is well known as a Hopf bifurcation, while Fig. 2(b) to a quasi-periodic bifurcation.

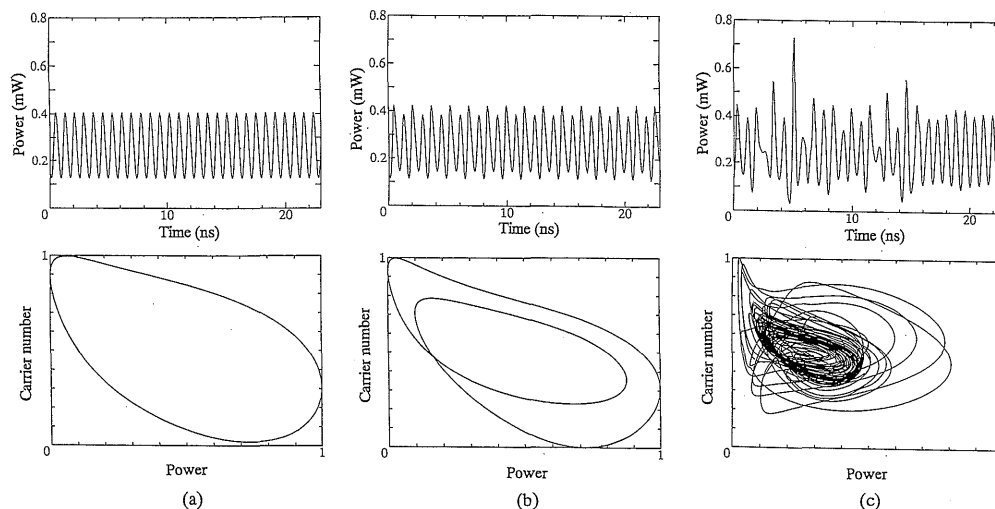


Fig. 3. Calculated laser output powers and their attractors at $J=1.06J_{th}$ and $L=18$ cm. (a) period-one oscillation at $r=1.6\%$, (b) period-two oscillation at $r=1.8\%$, and (c) chaotic oscillation at $r=2.0\%$.

In Fig. 2(a), the laser output stays stable for small external reflectivity, and it becomes period-one oscillation for small but not negligible external reflectivity. In period-one oscillations, the period is usually very close to the relaxation oscillation frequency of the solitary laser, but it is not always exactly the same.^{24–26} With increase of the external reflectivity, it bifurcates and finally evolves into chaotic oscillations. In Fig. 2(b), similar bifurcation to chaotic oscillations is observed, but period doubling bifurcation is not clearly visible and it evolves into chaotic oscillations directly after period-one oscillation. So it is called quasi-periodic bifurcation. In either case of chaotic oscillations, the laser output power shows irregular time variations with a scale of over nano-second. Totally, the noise of the laser power is much enhanced in this case. Lyapunov exponents are useful measures for stable or unstable nature in a chaotic system under a certain parameter condition. For fixed and periodic oscillations, the maximum value of Lyapunov exponents is less than zero and such a state is stable. On the other hand, it has positive value for chaotic oscillations and the system becomes unstable.

Figure 3 shows some numerical examples of the laser output powers and their attractors. The injection current and the external length are fixed to be $J=1.06J_{th}$ and $L=18$ cm, respectively. Figures 3(a) and (b) correspond to period-one and period-two oscillations at the external reflectivities of 1.6 and 1.8%, respectively. The frequency of period-one oscillation is close to the relaxation oscillation frequency of the solitary laser but it is not always equal to it. In the detailed analysis, it changes with the system parameters. Figure 3(c) shows a chaotic laser output power at the external reflectivity of 2.0%. From the attractor, it is easily seen that the state corresponds to chaos. The trajectory of the attractor is compact but the chaotic dimension is rather high. This reflects the fact that the system is described by the delay differential

forms as shown in Eqs. (4)–(6). Namely, due to a large degree of freedom introduced by the delay differential effect, the chaos in this system is a high dimension. At this state, the output power contains much noise and the optical spectrum is broadened. It is not easy to observe the waveform of the laser output power directly since the time scale of the output power variations is very high. But the periodic or chaotic behaviors can easily be observed by an optical spectrum such as taken by a Fabry-Perot interferometer. In fact, we can observe the growth of a spectral peak corresponding to the relaxation oscillation frequency for a period-one oscillation. With further increase of the external reflectivity, the output power shows quasi-periodic oscillations and we can observe an external mode frequency peak and its higher harmonics in the optical spectrum beside of the relaxation oscillation frequency. In strict sense, the additional spectral frequency appeared in the optical spectrum in a quasi-periodic oscillation is not exactly equal to the frequency calculated from the external cavity length due to the non-linear nature of the system. The maximum Lyapunov exponent is one of measures for chaotic dynamics as already stated. For example, the value of the maximum Lyapunov exponent such as in Fig. 3(c) is positive, then, the system is proved to be chaotic. On the other hand, it stays a stable state for a negative value as shown in Fig. 3(a). Another measure for chaotic dynamics is a chaos dimension and it is used to distinguish between chaotic irregularity and random noise. But we need a large number of data to calculate the dimension and it is not easy to evaluate for actual experimental data due to the presence of stochastic noise.

3.2 Long Range Chaotic Dynamics

One of well known effects in the presence of external optical feedback in semiconductor laser is output power jumps for increase of the injection current.²⁷ Figure 4(a) shows such a case calculated from the rate equations.

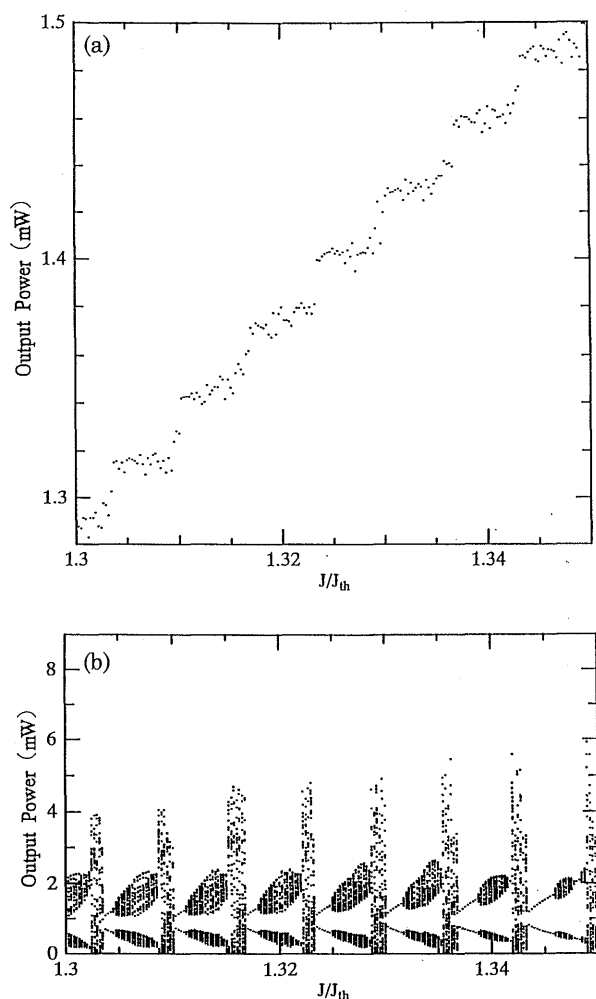


Fig. 4. (a) calculated output power jumps for increase of the injection current at $L=15$ cm and $r=1.0\%$. (b) bifurcations of the laser output power within the same current range as (a).

The external length and reflectivity are $L=15$ cm and $r=1.0\%$, respectively, which intrinsically corresponds to the regime III. The output power is proportional to the laser oscillation frequency and the amount of each output power jump is equal to that calculated from the external mode frequency. The jump of the output power is originated from the external mode alternation, namely, one external mode switches to the next at a jump position. We have demonstrated for the first time that there exists a chaotic scenario between successive jumps. Figure 4(b) shows bifurcations of the output power and periodic bifurcations of the output power between two successive jumps are observed. At the position after a mode jump, the laser oscillates with period-one, the laser becomes unstable with increase of the injection current, and, finally, it evolves into chaotic states. The frequency of period-one oscillation in the bifurcations is also the relaxation oscillation frequency and spectral peaks observed in quasi-periodic oscillations are also originated from the external mode. In the corresponding experiment, the L-I charac-

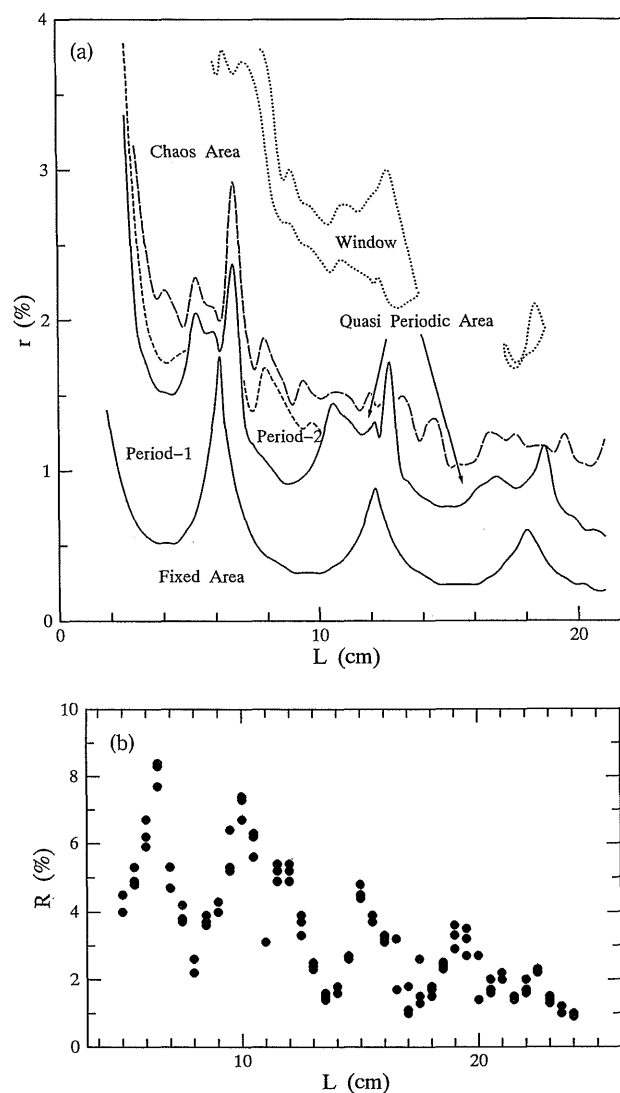


Fig. 5. (a) calculated phase diagram for boundaries of each state in bifurcations at $J=1.3J_{th}$. (b) experimentally obtained boundary between stable state and period-one oscillation at $J=1.5J_{th}$.

teristic in the presence of external optical feedback has a hysteresis. In the numerical simulations, the L-I characteristic was calculated as a step response for the injection current so that the laser output power is intrinsically calculated for the increase of the injection current. The chaotic scenarios were also investigated by the experiments and chaotic bifurcations were observed by optical spectra from a Fabry-Perot interferometer. The good coincidence between the experiments and the theoretical expectations was found.

Figure 5(a) shows a numerical result of the phase diagram for boundaries between each state in the bifurcations. The injection current is fixed to be $J=1.3J_{th}$. For example, the lower solid curve represents the boundary between fixed stable area and period-one state. From this figure, we can easily observe a periodic bifurcation at a certain external cavity position. The notable feature of

this graph is that critical reflectivity of the fixed stable state shows a periodic structure for variation of the external cavity length and the stable area is much enhanced at peak positions. At stability peaks (for example at $L=6.5$ cm), the output power stays stable for rather large external reflectivity, but it soon evolves into chaotic state through short range of quasi-periodic oscillations for increase of the external reflectivity. On the other hand, at stability bottoms (for example at $L=9.5$ cm), we can observe a typical period doubling bifurcation. The phase diagrams were also examined for other values of the injection current and it is found that the stable peak separation is a function of the injection current. Then, the period was proved to be exactly equal to the length calculated from the relaxation oscillation frequency of the solitary laser. Figure 5(b) shows the experimental result of the stability peak enhancement at $J=1.5J_{th}$.²⁸⁾ In the experiment, external reflectivity at which subpeak due to the onset of periodic bifurcation appeared in the optical spectrum observed by a Fabry-Perot interferometer was examined. It is noted here that the external mirror reflectivity in the experiments is not directly equal to or compatible with that in the theoretical one. Due to a small area of the laser active region and the diffraction effect by a collimating lens in front of the laser in the experiment, it is not easy to determine the actual fraction of the feedback power into the active region. The intensity reflectivity R in Fig. 5(b) is the reflectivity that takes into account of the external loss of the power for the laser light transmission and coupling losses due to such as the diffraction effect are not included.

The periodic structure of the stable state boundary and the enhancement of stable state are explained by the external mode competitions at near the relaxation oscillation frequency, which is based on the linear stability analysis in Sect. 2.3. For increase of the external reflectivity, the external mode near the relaxation oscillation frequency at first grows up and it leads to the laser instability. At stability peaks, two external modes are competing and the two linear modes do not exceed the instability threshold. As a result, rather long living stability for increase of the external reflectivity is privileged. But the output power soon destabilized once quasi-periodic oscillations start. On the other hand, at stability bottoms, only one external mode near the relaxation oscillation frequency concerns so that the laser output smoothly evolves into chaotic via period doubling bifurcation for increase of the external reflectivity. The relaxation oscillation frequency becomes undamped for increase of the external reflectivity. The relaxation oscillation frequency in the presence of external feedback (we here call a frequency at period-one oscillation as a "relaxation oscillation frequency" in the presence of external feedback) is also a function of the external cavity length. The relaxation oscillation frequency Ω is calculated based on the linear stability analysis as follows^{12,13)}:

$$\Omega^2 - \omega_R^2 = \frac{\Omega}{\tau_R} \cot\left(\frac{\Omega\tau}{2}\right). \quad (16)$$

It also has a periodic structure for increase of the external cavity length with a period equal to the length corresponding to the relaxation oscillation of the solitary laser.²⁹⁾ Namely, the relaxation oscillation decreases as increase of the external cavity length, it suddenly jumps up at stability peaks in Fig. 5(a), and repeats similar process.

3.3 Short Range Chaotic Dynamics

There exists short range dynamics of the output power in semiconductor lasers with optical feedback. Here, "short range" means small change of the external mirror position compatible with optical wavelength λ .³⁰⁻³⁵⁾ It is well known that a periodic undulation is observed in the laser output power with a period equal to half of the wavelength for small change of the external mirror position. Figure 6(a) shows such an undulation at $J=1.3J_{th}$ and $r=7\%$. Figure 6(a) is rather for a large optical feedback case. In general, sinusoidal undulation with small amplitude is observed for small reflectivity. With increase of the external reflectivity, clear periodic structure is visible and sudden drops in the waveform with period equal to $\lambda/2$ as shown in Fig. 6(a) are observed. The periodic undulation for small change of the external mirror position has already been well known. But, surprisingly, it is found that, within each period, chaotic scenario is also involved.³⁶⁾ Figure 6(b) shows bifurcations of the laser output power corresponding to Fig. 6(a). In Fig. 6(b), at around $L=4.2000$ cm, the laser output power shows chaotic variations and it reduces to periodic and stable oscillations for increase of the external cavity length. The similar process is repeated with a period equal to $\lambda/2$. In actual experimental situation, there is also a hysteresis either for increase or decrease of the external cavity position. The numerical simulations were done for the increase of the external cavity length. Figure 6(c) shows experimental results of optical spectra for small change of the external cavity position. The offset of the external cavity length is 4.2 cm and the external intensity reflectivity is $R=2\%$ and the injection current is $J=1.3J_{th}$. The external cavity length is increased from bottom to top in the optical spectra. In this figure, unstable state (weak chaotic or quasi-periodic oscillation) reduces to periodic oscillation and to stable state, then it again becomes unstable oscillations with a period equal to $\lambda/2$. For example, the spectrum at $\Delta L=1 \mu\text{m}$ is somewhat destroyed and corresponds to a weak chaotic state.

Up to now, we assume a single internal mode oscillation for a semiconductor laser. But, for large external feedback reflectivity, a semiconductor laser sometimes oscillates with multi-modes. In such a case, we observe periodic undulations with periods not only $\lambda/2$ but also $\lambda/4$, $\lambda/6$, and so on, for small change of the external cavity length. Which period occurs in the laser output power variations depends on the absolute external mirror position from the laser facet.^{27,37)} For long range of the external cavity variations equal to the order of \sim mm or more, there also exists periodic change of the laser output power.

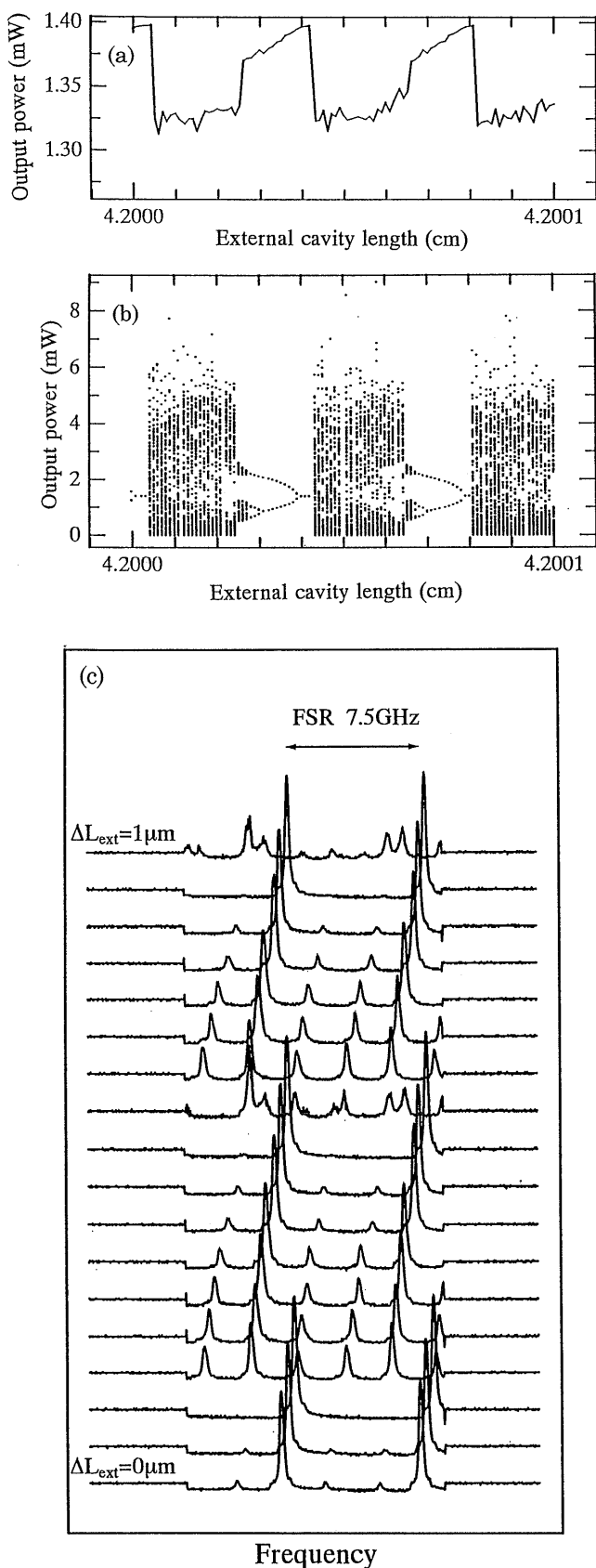


Fig. 6. (a) calculated undulation of the laser output power with period equal to $\lambda/2$ at $J=1.3J_{\text{th}}$ and $r=7\%$. (b) bifurcation of the laser output power corresponding to (a).

er with a period equal to the effective internal cavity length when the laser oscillates with multi-modes. At moderate optical feedback, when only one internal mode is related to the laser oscillation (which occurs at integer multiples of the internal cavity length $m\eta l$; m and η being an integer number and the effective refractive index of the laser medium), an undulation with period $\lambda/2$ is observed. When two internal modes are related to the laser oscillation (at $(m+1/2)\eta l$), an undulation with period $\lambda/4$ is observed. Similarly, higher order periodic undulations are observed depending on the external mirror position and the excited internal modes. Even in a higher order periodic undulation, there exist chaotic bifurcations within that period.³⁷⁾ Those effects are well demonstrated by the numerical simulation of the multi-mode laser rate equations and can be compared with the experimental results.

3.4 Low Frequency Fluctuations

The instability of semiconductor laser with optical feedback is much enhanced with increase of the external mirror reflectivity or length, which can be easily recognized from the increase of the parameter value C in Eqs. (12) and (13). The laser becomes unstable when the value C has a larger value than unity and many modes (external-cavity modes and antimodes) are excited depending on the parameter conditions. Among many modes, a laser usually oscillates with a maximum gain mode for a low external reflectivity, however, it sometimes destabilized due to a large value of C and drifts or slippings between successive modes occur.³⁸⁻⁴¹⁾ At this state, the laser is suddenly trapped to an antimode on its way to reaching the maximum gain mode. It is brought back to the solitary laser state in an instant and the sudden output power drop occurs. Then the laser starts drifts and the process repeats all over again. This process is explained by a saddle node instability in the system. The well known effects of the mode slippings are pulsations and low frequency fluctuations (LFFs) of the laser output power and the effects are related to the coherence collapse of the laser oscillation. Figure 7 shows examples of low frequency fluctuations at $L=30$ cm. The fraction of the external feedback was several percents in intensity. Low frequency fluctuations are phenomena of sudden power drops of the laser output power whose frequency is typically from several MHz to the order of tens of MHz. Figure 7 shows the dependence on the injection currents at $J=1.28J_{\text{th}}$, $1.20J_{\text{th}}$, and $1.10J_{\text{th}}$ from (a) to (c), respectively. At first, low frequency fluctuation was recognized in a low injection current near the laser threshold, but, recently, it was also observed in rather high injection current.⁴²⁾ Therefore, low frequency fluctuation is a universal phenomenon in semiconductor lasers with optical feedback. The waveforms as shown in Fig. 7 are obtained as low pass filtered signals less than 1 GHz. If we use a fast response detector that has a resolution as fast as picosecond or more, we can observe trains of pulsation signals in the waveform when low frequency fluctuations occur. Since low frequency fluctuation is originated from

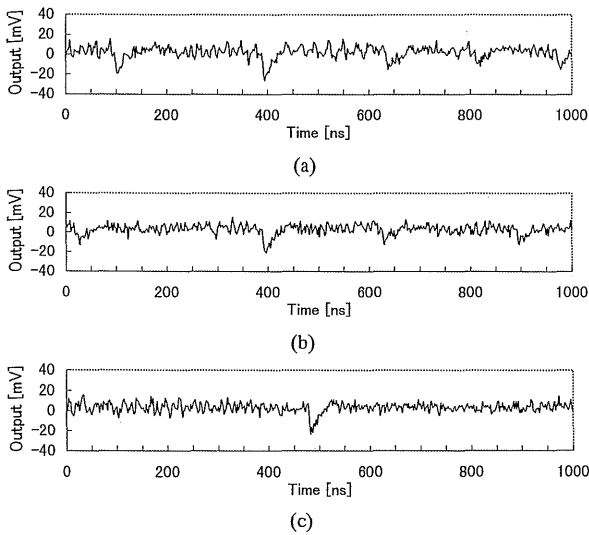


Fig. 7. Experimentally obtained low frequency fluctuations at $L=30$ cm. The fraction of the external feedback was several percents in intensity. Injection currents are (a) $J=1.28J_{th}$, (b) $1.20J_{th}$, and (c) $1.10J_{th}$.

unstable saddle node instability, the laser output power can be easily locked to a periodic oscillation by a modulation for the injection current with a frequency near the external cavity mode, which is similar to the idea of chaos control to an unstable periodic orbit as discussed in the following.⁴³⁾ Low frequency fluctuations are observed not only for a single internal mode oscillation but also for a multi-mode oscillation.

3.5 Coherence Collapse

When low frequency fluctuations present in the output power, the laser sometimes oscillates multi-modes and the coherence is much destroyed. The state is known as coherence collapse. Coherence collapse is not always led by low frequency fluctuations of the laser output power, but low frequency fluctuation is one of the important route to coherence collapse. At a coherence collapse state, even if the laser looks like to be oscillated as a single internal mode observed by such as a spectrum analyzer with THz resolution, the spectrum observed by a Fabry-Perot interferometer with narrow spectral range is completely destroyed. In this case, we cannot observe output power jumps such as shown in Fig. 4(a) and the output power is linearly proportional to the injection current as shown in Fig. 8(a). Figure 8(a) is the experimental result, and the length and intensity reflectivity of the external cavity were $L=15$ cm and $R=3\%$, respectively. The corresponding optical spectrum observed by a Fabry-Perot interferometer is shown in Fig. 8(b). We cannot distinguish any spectral peaks in this state. The L-I characteristics in Fig. 8(a) is a static nature (equivalently the mean intensity) and, as for the dynamic characteristics, the laser output power shows chaotic oscillations throughout the range of the injection current. In general, coherence collapse occurs in the regime IV of the external reflectivity discussed in the introduction, but it oc-

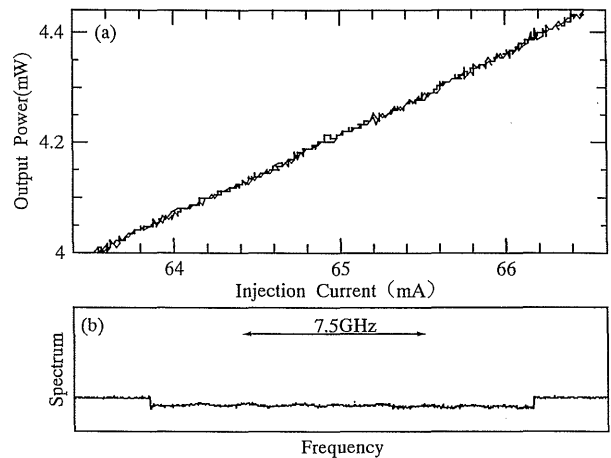


Fig. 8. Experimentally obtained (a) L-I characteristics and (b) optical spectrum observed by a Fabry-Perot interferometer at coherence collapse state. Length and intensity reflectivity of the external cavity are $L=15$ cm and $R=3\%$.

curs depending on the system parameters and happens even at a low external reflectivity. As a general trend, the instability is much enhanced either for long external cavity length or low bias injection current. Then, the coherence collapse is easily observed at the regime IV at low bias injection current with long external cavity length.

3.6 Phase Conjugate Optical Feedback

Recently, a semiconductor laser is frequently used as a light source in phase conjugate optics. The dynamic characteristics of phase conjugate optical feedback in semiconductor lasers are interesting issues not only from the fundamental physical study but also from the applications. There are many subjects for the study of the dynamics in semiconductor lasers with phase conjugate optical feedback. We here consider a degenerated four wave mixing phase conjugate feedback with a fast time response such like from a Kerr medium.⁴⁴⁻⁴⁸⁾ Other cases of the effects for phase conjugate feedback will be briefly described in later. The main difference between conventional optical mirror feedback and phase conjugate feedback is the phase θ in Eqs. (4) and (5) and the phase is written by taking the nature of the phase conjugate mirror into consideration as follows⁴⁴⁾:

$$\theta(t) = \phi_{PCF} + \phi(t) + \phi(t - \tau), \quad (17)$$

where ϕ_{PCF} is a constant phase change by the phase conjugate mirror reflection. The notable feature of the phase is that it is locked to a certain value with time evolution, while the phase for the case of conventional optical feedback is linearly increased with time. Other different point derived from this fact is that the stationary solution for the phase is uniquely defined due to the phase locking. In conventional optical feedback, multiple stationary phase solutions in Eq. (12) induce many antimodes and this results in saddle node instability and low frequency fluctuations in the laser output power. On the other hand, such instability is not observed for phase conjugate feed-

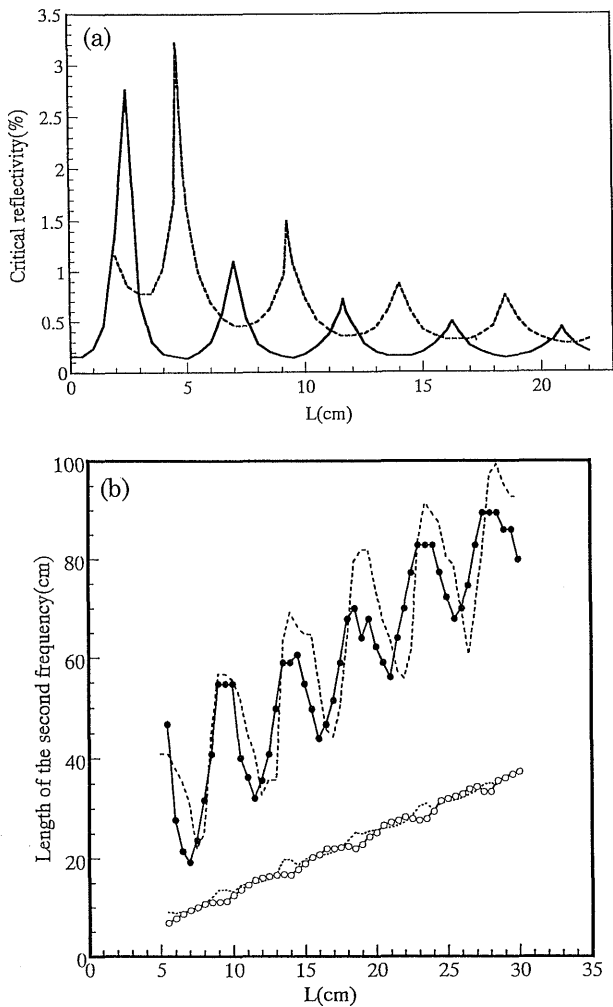


Fig. 9. (a) calculated boundary between stable state and period-one oscillation at $J=1.5J_{th}$. Solid line is the boundary for the case of phase conjugate feedback and dotted line for conventional optical feedback. (b) length corresponding to the excited frequency due to the external mode for the external cavity length at $J=1.5J_{th}$. Open and closed circles are for conventional and phase conjugate feedback calculated by the linear stability analysis, respectively. Dotted lines are calculated results directly from the rate equations.

back since there exists no antimode. Therefore, different dynamics from the case of conventional optical feedback are observed for phase conjugate feedback.

One of different dynamic behaviors is plotted in Fig. 9(a). The boundary between stable state and period-one oscillation is numerically calculated by the linear stability analysis at $J=1.5J_{th}$. Solid line is the boundary for the case of phase conjugate feedback and dotted line for conventional optical feedback which is already shown in Fig. 5(a). Periodic stability enhancement is observed with a period equal to a length corresponding to the relaxation oscillation frequency of the solitary laser, but stability peaks between the cases of phase conjugate and conventional optical mirrors are located alternately with each other. For increase of the external reflectivity, a frequency related to the external mode is excited beside of

the relaxation oscillation frequency. In conventional optical feedback, the excited frequency in the optical spectrum is nearly equal to one for the external cavity mode (but not exactly equal to it due to the nonlinear nature of the phenomena). Open circles in Fig. 9(b) show the relation for conventional optical feedback at $J=1.5J_{th}$. However, the behavior for phase conjugate feedback is completely different from that of conventional optical feedback. Closed circles in Fig. 9(b) shows the result for the phase conjugate optical feedback. The frequency excited by the external cavity is quite different from the external mode frequency and it has a periodic structure with a period equal to the relaxation oscillation frequency of the solitary laser again. In the figure, open and closed circle data are calculated from the linear stability analysis and the dotted curves correspond to direct numerical simulations from the rate equations.

As already mentioned, there exist several subjects for the study of the dynamics in semiconductor lasers with phase conjugate optical feedback. One of them is the dynamics for phase conjugate feedback generated from a non-degenerated four wave mixing. In that case, one more parameter, i.e., the phase mismatch, is introduced and the system shows somewhat different dynamics compared with the case for a degenerated four wave mixing.^{49,50} Another issue of phase conjugate feedback is the time response of a phase conjugate mirror. As the time scale of the dynamics in a semiconductor laser with optical feedback is nano-second or faster, the effect of finite time must be considered in the dynamics for a phase conjugate mirror with slow time response.^{51,52} For example, the time response of a photorefractive phase conjugate medium such as a photorefractive crystal is so slow compared with the time fluctuations of a semiconductor laser. So the grating formed in a photorefractive crystal can be considered as a static grating.⁵³ Once the grating is formed in a photorefractive crystal, the dynamics are only governed by the total feedback loop of the pump beam. As a result, the dynamics are completely the same as those for a conventional mirror feedback except for the generation of a spatial phase conjugate wave. The dynamics in such photorefractive phase conjugate feedback are quite different from those for a fast response phase conjugate mirror.

4. Chaos Control and Synchronization

Chaotic dynamics in optics have been studied for more than these two decades. Chaos and instability in many optical fields have attracted many researchers as a fundamental physical study. Chaos in optics in early times was an unwanted effect in applications since it enhances instability and noise in laser systems and other nonlinear optical systems. But, since early '90s, the situation has been changed. For example, several methods of chaos control algorithms were developed and they were successfully applied to laser systems to reduce laser noises. Other notable application of chaos is the chaos synchronization between two similar chaotic systems. It provides

the method of a secure communication system. In this section, the methods of chaos control and synchronization are discussed and their applications are demonstrated.

4.1 Chaos Control: The Method

The first method of chaos control was proposed by Otto, Grebogi, and Yorke in 1990, which is known as the OGY algorithm.⁵⁴⁾ By their control, the system is attracted to a certain unstable orbit such as a saddle node point by a very small perturbation to one of the system parameters when the system is in a chaotic state and very close to the attractor to be controlled. Then the original dynamic characteristics are not affected by the perturbation. The method was successfully demonstrated by numerical simulations. But the method is rather mathematical one and it is not easy to implement for actual experimental systems. The second method proposed by Pyragas is the continuous control method.⁵⁵⁾ The system outputs at times $t-T$ and t (where T is the delay and is chosen to be near or equal to the response time of the system) are detected and the difference between them is fed back to one of the system parameters. For example, in our case, choosing the injection current as a control parameter, the control signal is given by

$$J = J_b \left\{ 1 + \beta \frac{P(t-T) - P(t)}{P_0} \right\}, \quad (18)$$

where J_b is the bias injection current, β is the feedback gain, and P_0 is the average output power. The control signal is completely eliminated in those methods after the control is succeeded.^{56,57)} The third example of the chaos control is the OPF (occasional proportional feedback) method proposed by Hunt and Roy, and others.⁵⁸⁻⁶¹⁾ In chaos control, the important information to perform the control is not an amplitude of the control signal but the timing or phase of the waveform. The timing pulses which are very small compared with the system output are generated from the original output and they are applied to one of the control parameters as small perturbations. Then the system with chaotic oscillation is attracted to usually a periodic cycle. This method was successfully applied to a solid state laser system and noise in the laser output power was much reduced. The OPF method requires some digital electronic circuits to generate a control signal. Therefore, it is not easy to implement for very fast time varying signals in spite of very suitable method for actual experimental situations. As an alternative method for chaos control, we have proposed a sinusoidal modulation for a fast time varying signal which is applicable to semiconductor lasers.

4.2 Chaos Control and Noise Suppression in Semiconductor Laser

The idea of the sinusoidal modulation for one of the control parameters is that the system may be attracted to a periodic or stable state by the control with a rather small periodic perturbation even if the system is a little bit far from the basin of the targeted attractor, which is the most probable case in experiments.^{62,63)} One of the

problems is how to choose a modulation frequency. The other one is that the attractor of the original dynamics may be destroyed and changed by the modulation. In the following, we introduce the method of the sinusoidal modulation for the injection current and show some results.^{11,64)} The modulation depth must be small less than several percents of the bias injection current, but it was sometimes compatible with or over 10% in our experiments. The important thing is that, even in that case, the control was only succeeded for the chosen frequency and failed for other frequencies. So we can consider that the stability by the control is originated from the original system dynamics.

The stability of the laser output power in semiconductor laser with optical feedback is investigated by the linear stability analysis in Sect. 2.3. The imaginary part of a solution in Eq. (15) gives a frequency of a stable or unstable oscillation in the original system. Therefore, we use this frequency as a control parameter. By choosing the injection current as a control parameter, the sinusoidal modulation is applied as follows;

$$J = J_b \{ 1 + a_m \cos(2\pi f_m t) \}, \quad (19)$$

where f_m is the frequency determined from one of the linear modes and a_m is the amplitude of the modulation which must be small enough. Whether the control may go well or not depends on the extent of the basin of the attractor for that frequency. Figure 10 shows an example of the controls at the parameter values of $J = 1.1J_{th}$, $r = 1.5\%$, and $L = 25.5$ cm. The control frequency and amplitude are 1.25 GHz and $m = 0.021$, respectively. A chaotic waveform in Fig. 10(a) is controlled to a period-one oscillation as shown in Fig. 10(b) and noise of the laser output power in low frequency region is much reduced. The parameter values for the control are chosen as for the best control. The method is rather robust and a finite range of the parameter value exists for successful control, for example, the control is succeeded within the range of several tens to a hundred of MHz around the chosen frequency, but the extent of the attractor (the amplitude of the oscillation) after the control was varied depending on the modulation frequency and amplitude.

The method of chaos control proposed here can be applied to the noise suppression in the laser output power. Figure 11 shows a numerical result for the noise suppression by the proposed chaos control at $L = 15$ cm, $J = 1.3J_{th}$, and $r = 2.5\%$. In this case, the modulation frequency is taken to be $f_m = 2.38$ GHz and the modulation depth is $m = 0.0346$. However, the actual modulation depth that takes into account for the laser threshold becomes $mJ_b / (J_b - J_{th}) = 0.150$. This modulation depth may not be small in a sense of chaos control with negligible perturbation. In Fig. 11, the RIN in the lower frequency region less than 1 GHz is increased more than 20 dB/Hz (dashed line) in the presence of the external optical feedback compared with the solitary laser level (solid line). Then, by the control, the noise level is lowered as

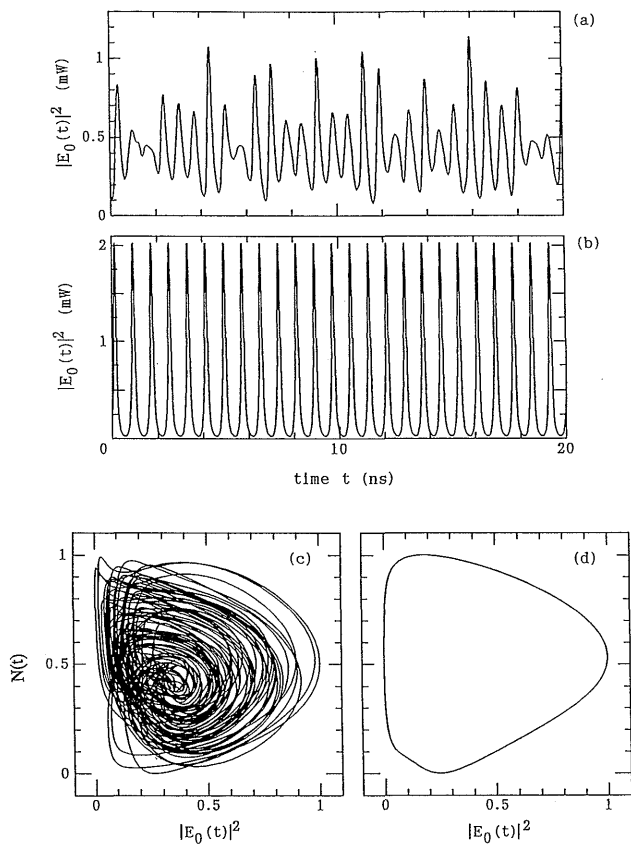


Fig. 10. Chaos control at the parameter values of $J=1.1J_{th}$, $r=1.5\%$, and $L=25.5$ cm by the numerical simulations. Control frequency and amplitude are 1.25 GHz and 2.1%. (a) original chaotic laser output and (b) after the control. (c) and (d) are the attractors corresponding to (a) and (b), respectively.

much as 10 dB/Hz (dotted line).

In actual, a high frequency injection current modulation has been employed to suppress feedback induced noise in semiconductor laser in optical data storage systems based on the empirical basis.^{65,66} However, the modulation depth is much larger than that of our method and a laser is sometimes brought below the threshold by the modulation. The modulation frequency is also determined empirically in those systems. Experimental verification of the proposed chaos control here is now under way. The problem is how to determine the modulation frequency in actual experiments since the exact device parameters for a semiconductor laser used must be specified in advance. In our preliminary experiments, by carefully choosing the state of chaos in the laser output power, the control was succeeded with certain integer multiples of a frequency which is very close to the external cavity mode.⁶⁷ But the modulation depth was still large (for example, around $m=0.1$) and the controlled modes were rather higher periodic states.

Recently, self-oscillating laser is interested as a future device in a DVD source in optical data storage systems. It can oscillate without an injection current modulation in the presence of external optical feedback due to satura-

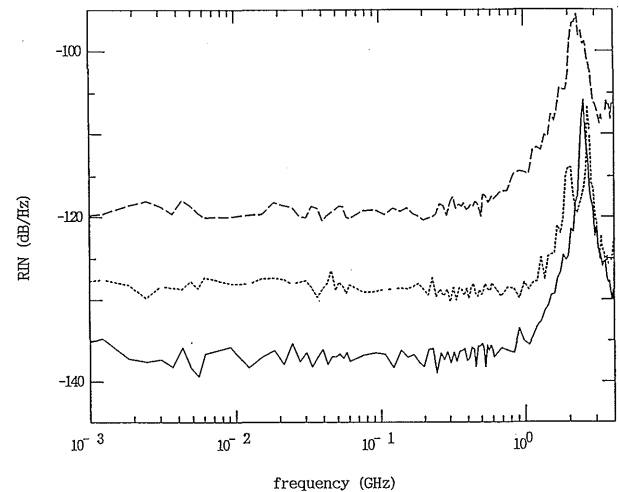


Fig. 11. Numerical result for the noise suppression by the chaos control at $L=15$ cm, $J=1.3J_{th}$, and $r=2.5\%$. Modulation frequency is taken to be $f_m=2.38$ GHz and the modulation depth is $m=0.0346$. Solid line: solitary laser, dashed line: with optical feedback, and dotted line: after the control.

ble absorber installed in the laser active region.⁶⁸ The chaos control algorithm introduced here may give an important information to design such a device. The injection current is not only a control parameter in our chaos control. Equivalently, direct optical modulation may be one of possible ways to control chaos. We have proposed such a control by introducing an extra external mirror in the optical path as a control mirror,⁶⁹ but the situation was not so simple in this case since the dynamics is much complicated compared with a single mirror case.^{70,71} Anyway, the control was sometimes successful in that system, but the original dynamics was considerably changed due to a large modulation depth.

4.3 Chaos Synchronization and Chaos Communications

Chaos synchronization is another topic that interests many researchers. In two similar chaotic systems, two outputs may be synchronized with each other, when chaotic signal from one of them is transmitted to the other.⁷² In optics, synchronization of chaotic laser systems was successfully demonstrated in solid state lasers and CO₂ lasers.^{73,74} Since the time scales of the phenomena are the order of microsecond in those laser systems and it is very easy to observe the waveforms electronically. To realize chaos synchronization, parameter values of two systems must be chosen close enough, however they must not always be exactly equal with each other. Chaos synchronization is rather robust and the effects of parameter mismatch for successful synchronization were studied. The allowance of the parameter mismatch depends not only on a system employed but also the values of the system parameters and it ranges from several percent to tens of percents for the original parameter values. By using two feedback induced chaotic systems in semiconductor lasers as a transmitter and a receiver, chaotic synchronization can be achieved.^{75,76} But the external

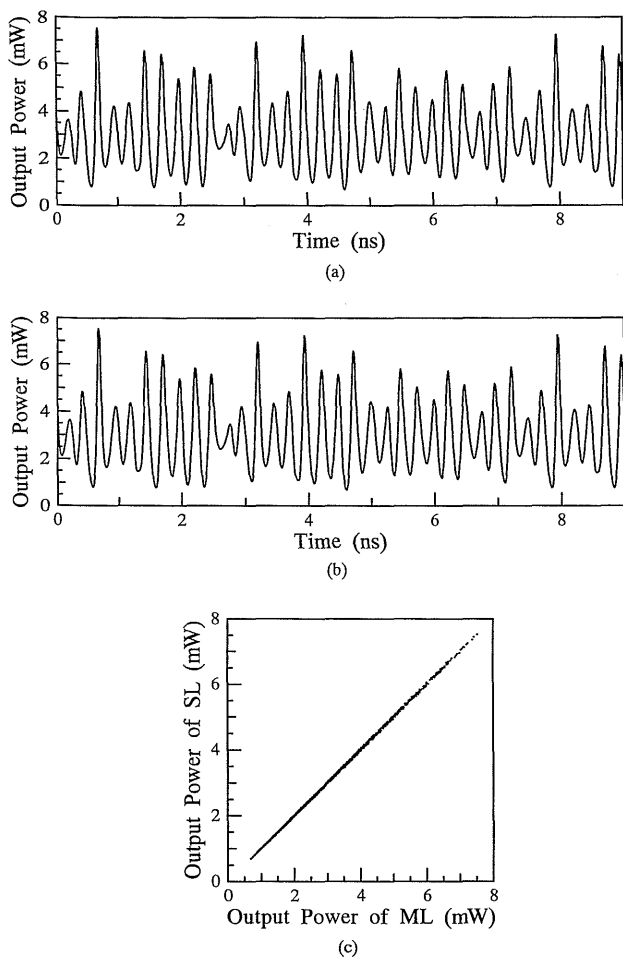


Fig. 12. Numerical result of chaos synchronization. Laser output powers of the transmitter (a) and the receiver (b). (c) correlation plot between the output powers of the transmitter (horizontal axis) and the receiver (vertical axis). Time offsets are taken arbitrary. External mirror reflectivity in the transmitter is 2% and amount of the optical injection to the receiver is 2%. The control mirror in the receiver system is not presented.

mirror to introduce optical feedback in the receiver system may not be always required to realize chaos synchronization, because the laser can be synchronized simply by the injection locking from an external light.⁷⁷ Figure 12 shows a numerical result of chaos synchronization for such a case. Figures 12(a) and (b) are chaotic waveforms of the transmitter and receiver, respectively, and Fig. 12(c) is the correlation plot between the two waveforms. The time offsets in the figure are taken arbitrary. In Fig. 12, the two lasers operate under almost the same parameter conditions and the external mirror reflectivity in the transmitter was 2%. The amount of the optical injection to the receiver was 2%. However, the synchronization was succeeded within the injection range from 1 to 2%.

Chaos synchronization can be used for secure communications. Even though the method of chaos synchronization has a robustness, it is not easy to syn-

chronize chaotic systems without knowing the system and the values of the system parameters. It is also not easy to reconstruct chaotic attractor at a receiver site without knowing such information. Namely, using system parameters as keys, chaotic communications are realized with high security. In actual, Goedgebuer *et al.*^{78,79} has proposed chaotic communication systems and done some experiments. The system is an opto-electronic feedback one and is composed of a semiconductor laser source with nonlinear wavelength control feedback to the injection current. They have transmitted a piece of music and successfully reconstructed it. In the system, the message to be transmitted was superimposed with the injection current to the semiconductor laser in the transmitter and the signal level was about one-hundredth of the chaotic variations. For such a small transmitted message, the laser output of the receiver system only reproduces chaotic variations equal or similar to the transmitter. Then, subtracting the receiver signal from the transmitter signal, the message is reproduced. Their system is an opto-electronic hybrid system so that the bandwidth is limited by the time response of the electronic circuits. Roy *et al.* proposed a chaotic communication system which consists of EDFA (erbium-doped fiber amplifier) nonlinear feedback loops and realized 126 Mbits/s data transmission.⁸⁰

5. Other Topics and Applications of Chaos

Various types of semiconductor lasers have been proposed up to now. Chaotic dynamics in semiconductor lasers discussed here are also applicable to those lasers as far as the dynamics are described by the same laser rate Eqs. (4)–(6). The same or similar chaotic dynamics are expected for Fabry-Perot bulk laser, MQW laser, or DFB laser, though the phenomena depend on specific structures of lasers or device parameters. But, for other types of semiconductor lasers such as VCSELs, the dynamics become somewhat different from above lasers since the rate equations must include spatial and polarization effects. The internal reflectivity of light in the laser cavity in VCSELs is very high as much as 99% or more. But the short internal cavity length makes the external feedback effects significant. The optical feedback effects in VCSELs have been studied by several researchers.^{81–84} In the applications of VCSELs, for example, a VCSEL array in integrated optical circuits for interconnect, the feedback effects may be an important issue in the actual fabrication of the system. Since the device structure of VCSELs is much different from other lasers and the internal intensity reflectivity is much higher than other semiconductor lasers, different dynamics are observed and the study is now under way. Also the dynamics is somewhat related to other micro-cavity lasers. Furthermore, chaos in such a small space is also related to quantum chaos⁸⁵ and fruitful results are expected in this area.

Another important area of chaotic dynamics is high power lasers. Strictly speaking, a laser field depends not

only on time but also on space, so that the laser rate equations must include spatial differential terms. When the laser field is restricted in a small area or equivalently it is assumed constant for space, the Eqs. (4)–(6) are valid. But, for a broad area laser or a flared laser, we must take the spatial effects into consideration. These lasers have been developed to attain high power semiconductor lasers. These lasers themselves are intrinsically unstable in time and space without any other external modulation and optical injection since they include spatial effects. The dynamic behaviors for these lasers are also an important issue from the fundamental study of laser instability and chaos. Fisher *et al.* have done several investigations for the dynamic behaviors of broad area lasers and demonstrated spatio-temporal dynamics in the laser output power.^{86,87} The control of the laser output power in a broad area laser was also proposed based on optical feedback.^{88,89} A flared semiconductor laser has a tapered resonator structure and the device is fabricated for a high power laser. It also shows chaotic dynamics without external disturbances.⁹⁰ The control of the laser output power has been proposed by a simple injection current modulation and a continuous control similar to the Pyragas method discussed in Sect. 4.1.⁹¹ Another type of high power semiconductor laser is a laser diode array.^{92–94} Totally high power laser is attained by such a device, but the problem is that each laser in array emits light independently or with a little correlation. Therefore, it is difficult to totally obtain a high intensity and a coherent beam. Sometimes it shows chaotic dynamics when lasers among array are coupled with each other. A laser array coupled with neighborhood elements can be described by a coupled map lattice equations which lead to well known chaotic spatio-temporal dynamics. To control the laser and obtain a high quality beam, the control methods introduced here may give important information.

Another topics of the applications of feedback induced chaos in semiconductor lasers are internal mode selection by chaotic search,^{95–97} linewidth controlling,^{98–100} interferometer stabilization,¹⁰¹ and heterodyne detection of chaotic signals.⁶³ The details of each topics are found in the literature.

6. Conclusions

This paper provided the phenomena of feedback induced instability and chaos in semiconductor lasers and its recent applications based on chaos control and synchronization. The study of the noise effects is still an important issue in semiconductor lasers and the irregularity of the output power was explained and understood by the chaotic behaviors. Stability and instability natures of the output power in semiconductor lasers with optical feedback are important not only for the fundamental study but also for system designs by using them as a light source. Recently, a variety of device structures for semiconductor lasers have been proposed and the dynamic behaviors for them in the presence of optical feedback have

been investigated. The chaotic dynamics of Fabry-Perot lasers were studied for these two decades and they were understood for some extent. But a lot of issues have still been left as future problems to be investigated, for example, the origin of low frequency fluctuations concerning to one of the routes to chaos in semiconductor lasers with optical feedback is not fully understood. On the other hand, a little is known for the dynamics of new lasers such as VCSELs and broad area lasers in the presence of feedback. The study for the applications of chaos is started very recently and we have shown some examples of recent researches. Fruitful results are expected in these area since the optics is very fast in time and has parallelism of the processing in nature. The discussion here will give important information for other studies of instability and chaos in the field of optics such as in micro-cavity systems and other nonlinear optical devices.

Acknowledgment

The author would like to thank Y. Liu, P. Davis and A. Murakami for stimulating discussion.

References

- 1) H. Haken: *Phys. Lett.* **53A** (1975) 77.
- 2) K. Ikeda: *Opt. Commun.* **30** (1979) 257.
- 3) R. Lang and K. Kobayashi: *IEEE J. Quantum Electron.* **QE-16** (1980) 347.
- 4) G.H.M. van Tartwijk: Ph.D. Thesis, Vrije University (1994).
- 5) G.H.M. van Tartwijk and G.P. Agrawal: *Prog. Quantum Electron.* **22** (1998) 43.
- 6) R.W. Tkach and A.R. Chraplyvy: *IEEE J. Lightwave Technol.* **4** (1986) 1655.
- 7) J. Sacher, W. Elsässer and E.O. Göbel: *IEEE J. Quantum Electron.* **27** (1991) 373.
- 8) R. Binder and S.W. Koch: *Prog. Quantum Electron.* **19** (1995) 307.
- 9) K. Petermann: *Laser Diode Modulation and Noise* (Kluwer Academic, Dordrecht, 1988).
- 10) G.P. Agrawal and N.K. Dutta: *Semiconductor Lasers* (Van Nostrand Reinhold, New York, 1993).
- 11) Y. Liu, N. Kikuchi and J. Ohtsubo: *Phys. Rev.* **E51** (1995) R2697.
- 12) B. Tromborg, J.H. Osmundsen and H. Olesen: *IEEE J. Quantum Electron.* **QE-20** (1984) 1023.
- 13) A. Murakami, J. Ohtsubo and Y. Liu: *IEEE J. Quantum Electron.* **33** (1997) 1825.
- 14) D. Lenstra: *Opt. Commun.* **81** (1991) 209.
- 15) Y. Cho and T. Umeda: *Opt. Commun.* **59** (1986) 131.
- 16) J. Sacher, D. Baums, P. Panknin, W. Elsässer and E.O. Göbel: *Phys. Rev.* **A45** (1992) 1893.
- 17) P. Besnard, B. Meziane and G.M. Stephan: *IEEE J. Quantum Electron.* **29** (1993) 1271.
- 18) Y. Kitaoka, H. Sato, K. Mizuuchi, K. Yamamoto and M. Kato: *IEEE J. Quantum Electron.* **32** (1996) 822.
- 19) C. Masoller and N.B. Abraham: *Phys. Rev.* **A57** (1998) 1313.
- 20) J. Mørk, J. Mark and B. Tromborg: *Phys. Rev. Lett.* **65** (1990) 1999.
- 21) J. Ye, H. Li and J.G. McInerney: *Phys. Rev.* **A47** (1993) 2249.
- 22) H. Li, J. Ye and J.G. McInerney: *IEEE J. Quantum Electron.* **29** (1993) 2421.
- 23) A. Ritter and H. Haug: *J. Opt. Soc. Am.* **B10** (1993) 145.
- 24) J.S. Cohen, R.R. Drenten and B.H. Verbeek: *IEEE J. Quantum Electron.* **24** (1988) 1989.

- 25) J. Helms and K. Petermann: *IEEE J. Quantum Electron.* **26** (1990) 833.
- 26) A.M. Levine, G.H.M. van Tartwijk, D. Lenstra and T. Erneux: *Phys. Rev.* **A52** (1995) 3436.
- 27) H. Kakiuchida and J. Ohtsubo: *IEEE J. Quantum Electron.* **30** (1994) 2087.
- 28) S.Y. Ye and J. Ohtsubo: *Opt. Rev.* **5** (1998) 280.
- 29) C. Masoller: *Opt. Commun.* **128** (1996) 343.
- 30) J.W.M. Biesterbos, A.J. den Boef, W. Linders and G.A. Acket: *IEEE J. Quantum Electron.* **19** (1983) 986.
- 31) J.P. van der Ziel and R.M. Mikulyak: *IEEE J. Quantum Electron.* **20** (1984) 223.
- 32) G.A. Acket, D. Lenstra, A.J. den Boef and B.H. Verbeek: *IEEE J. Quantum Electron.* **20** (1984) 1163.
- 33) D.R. Hjelme and A.R. Mickelson: *IEEE J. Quantum Electron.* **23** (1987) 1000.
- 34) Z.M. Chuang, D.A. Cohen and L.A. Coldren: *IEEE J. Quantum Electron.* **26** (1990) 1200.
- 35) Y. Katagiri and S. Hara: *Appl. Opt.* **33** (1994) 5564.
- 36) Y. Ikuma and J. Ohtsubo: *IEEE J. Quantum Electron.* **34** (1998) 1240.
- 37) Y. Ikuma and J. Ohtsubo: *Proc. EOS Topical Meeting "Electromagnetic Optics"* (1998) 55.
- 38) J. Sacher, W. Elsässer and E.O. Göbel: *Phys. Rev. Lett.* **63** (1989) 2224.
- 39) G.H.M. van Tartwijk, A.M. Levine and D. Lenstra: *IEEE J. Quantum Electron.* **31** (1995) 466.
- 40) T. Sano: *Phys. Rev.* **A50** (1994) 2719.
- 41) I. Fischer, G.H.M. van Tartwijk, A.M. Levine, W. Elsässer, E. Göbel and D. Lenstra: *Phys. Rev. Lett.* **76** (1996) 220.
- 42) M-W. Pan, B-P. Shi and G.R. Gray: *Opt. Lett.* **22** (1997) 166.
- 43) Y. Takiguchi, Y. Liu and J. Ohtsubo: *Opt. Lett.* **23** (1998) 1369.
- 44) G.P. Agrawal and J.T. Klaus: *Opt. Lett.* **16** (1991) 1325.
- 45) G.P. Agrawal and G.R. Gray: *Phys. Rev. A* **46** (1992) 5890.
- 46) L.N. Langley and K.A. Shore: *IEEE Proc. Optoelectron.* **141** (1994) 103.
- 47) E. Bochove: *Phys. Rev. A* **55** (1997) 3891.
- 48) A. Murakami and J. Ohtsubo: *IEEE J. Quantum Electron.* **34** (1998) 1979.
- 49) G.H.M. van Tartwijk, H.J.C. van der Linden and D. Lenstra: *Opt. Lett.* **17** (1992) 1590.
- 50) G.R. Gray, D. Huang and G.P. Agrawal: *Phys. Rev. A* **49** (1994) 2096.
- 51) D.H. DeTienne, G.R. Gray, G.P. Agrawal and D. Lenstra: *IEEE J. Quantum Electron.* **33** (1997) 838.
- 52) W.A. van der Graaf, L. Pesquera and D. Lenstra: *Opt. Lett.* **23** (1998) 256.
- 53) Y. Tomita, R. Yahalom and A. Yariv: *Opt. Commun.* **73** (1989) 413.
- 54) E. Ott, C. Grebogi and J. A. Yorke: *Phys. Rev. Lett.* **64** (1990) 1196.
- 55) K. Pyragas: *Phys. Lett. A* **170** (1992) 421.
- 56) A.V. Naumenko, N.A. Loiko, S.I. Turovets, P.S. Spencer and K.A. Shore: *J. Opt. Soc. Am. B* **15** (1998) 551.
- 57) S.I. Turovet, J. Dellunde and K.A. Shore: *J. Opt. Soc. Am. B* **14** (1997) 200.
- 58) E.R. Hunt: *Phys. Rev. Lett.* **67** (1991) 1953.
- 59) R. Roy, T.W. Murphy, T.D. Maier, Z. Gills and E.R. Hunt: *Phys. Rev. Lett.* **68** (1992) 1259.
- 60) Y. Liu and J. Ohtsubo: *Opt. Lett.* **19** (1994) 488.
- 61) Y. Liu and J. Ohtsubo: *Opt. Rev.* **1** (1994) 91.
- 62) A.T. Ryan, G.P. Agrawal, G.R. Gray and E.C. Gage: *IEEE J. Quantum Electron.* **30** (1994) 668.
- 63) N. Watanabe and K. Karaki: *Opt. Lett.* **20** (1995) 1032.
- 64) N. Kikuchi, Y. Liu and J. Ohtsubo: *IEEE J. Quantum Electron.* **33** (1997) 56.
- 65) M. Ojima, A. Arimoto, N. Chinone, T. Gotoh and K. Aiki: *Appl. Opt.* **25** (1986) 1404.
- 66) G.R. Gray, A.T. Ryan, G.P. Agrawal and E.C. Gage: *Opt. Eng.* **32** (1993) 739.
- 67) S-Y. Ye and J. Ohtsubo: *Proc. JICAST'98/CPST'98* (1998) 218.
- 68) G.H.M. van Tartwijk and M.S. Miguel: *IEEE J. Quantum Electron.* **32** (1996) 1191.
- 69) Y. Liu and J. Ohtsubo: *IEEE J. Quantum Electron.* **33** (1997) 1163.
- 70) I. Fischer, O. Hess, W. Elsässer and E. Göbel: *Phys. Rev. Lett.* **73** (1994) 2188.
- 71) C. Simmendinger and O. Hess: *Phys. Lett. A* **216** (1996) 97.
- 72) L.M. Pecora and T.L. Carroll: *Phys. Rev. Lett.* **64** (1990) 821.
- 73) R. Roy and K.S. Thornburg: *Phys. Rev. Lett.* **72** (1994) 2009.
- 74) T. Sugawara, M. Tachikawa, T. Tsukamoto and T. Shimizu: *Phys. Rev. Lett.* **72** (1994) 3502.
- 75) V. Abbivazzu-Lodi, S. Donati and A. Sciré: *IEEE J. Quantum Electron.* **33** (1997) 1449.
- 76) C.R. Mirasso, P. Colet and P. Garcia-Fernandez: *IEEE Photonics Technol. Lett.* **8** (1996) 299.
- 77) J.K. White and J.V. Moloney: *Proc. NOLTA'97* (1997) 129.
- 78) J-P. Goedgebuer, L. Larger and H. Porte: *Phys. Rev. Lett.* **80** (1998) 2249.
- 79) L. Larger, J-P. Goedgebuer and F. Delorme: *Phys. Rev. E* **57** (1998) 6618.
- 80) G.D. Ban Wiggeren and R. Roy: *Science* **279** (1998) 1198.
- 81) J.Y. Law and G.P. Agrawal: *J. Opt. Soc. Am. B* **15** (1998) 562.
- 82) F. Robert, P. Besnard, M.L. Chares and G.M. Stephan: *IEEE J. Quantum Electron.* **33** (1997) 2231.
- 83) P.S. Spencer, C.R. Mirasso, P. Colet and K.A. Shore: *IEEE J. Quantum Electron.* **34** (1998) 1673.
- 84) J.V. Sandusky and S.R.J. Brueck: *IEEE J. Quantum Electron.* **33** (1997) 1574.
- 85) J.U. Nökel and A.D. Stone: *Nature* **385** (1997) 45.
- 86) H. Adachihara, O. Hess and E. Abraham: *J. Opt. Soc. Am. B* **10** (1993) 658.
- 87) J. Martín-Regalado, G.H.M. van Tartwijk, S. Balle and M. San Miguel: *Phys. Rev. A* **54** (1996) 5386.
- 88) W. Nagengast and K. Rith: *Opt. Lett.* **22** (1997) 1250.
- 89) K. Iida, H. Hisaki, O. Matoba, T. Omatsu, T. Shimura and K. Kuroda: *Opt. Commun.* **146** (1998) 6.
- 90) G. Levy and A.A. Hardy: *IEEE J. Quantum Electron.* **33** (1997) 26.
- 91) G. Levy and A.A. Hardy: *IEEE J. Quantum Electron.* **34** (1998) 1.
- 92) H.G. Winful and L. Rahman: *Phys. Rev. Lett.* **65** (1990) 1575.
- 93) M. Münke, F. Kaiser and O. Hess: *Phys. Lett. A* **222** (1996) 67.
- 94) D. Auerbach and J.A. Yorke: *J. Opt. Soc. Am. B* **13** (1996) 2178.
- 95) J. Mørk and B. Tromborg: *IEEE Photonics Technol. Lett.* **2** (1990) 21.
- 96) J. Mørk, M. Semkow and B. Tromborg: *Electron. Lett.* **26** (1990) 609.
- 97) Y. Liu and P. Davis: *Int. J. Bifur. Chaos* **8** (1998) (in press).
- 98) L. Goldberg, H.F. Taylor, A. Dandridge, J.F. Weller and R.O. Miles: *IEEE J. Quantum Electron.* **QE-18** (1982) 555.
- 99) P. Kurz and T. Mukai: *Opt. Lett.* **21** (1996) 1369.
- 100) B.W. Liby and D. Statman: *IEEE J. Quantum Electron.* **32** (1996) 835.
- 101) N. Watanabe and K. Karaki: *Opt. Lett.* **21** (1996) 1256.